Am J Cancer Res 2026;16(6):2215-2231
www.ajcr.us /ISSN:2156-6976/ajcr0170869

Original Article

Circ_0075829 affects POU5F1B expression through sponging miR-576-3p to promote growth, invasion, and angiogenesis of colon cancer cells

Huajun Fan[1], Yu Ding[2], Zhe Xiao[3], Shengbo Li[3], Yongbin Zheng[3]

[1]Department of Plastic Surgery, Renmin Hospital of Wuhan University, Wuhan 430060, Hubei, P. R. China; [2]Department of Pain, Renmin Hospital of Wuhan University, Wuhan 430060, Hubei, P. R. China; [3]Department of Gastrointestinal Surgery, Renmin Hospital of Wuhan University, Wuhan 430060, Hubei, P. R. China

Received December 19, 2025; Accepted May 9, 2026; Epub June 15, 2026; Published June 30, 2026

Abstract: Colon cancer represents a significant malignancy within the gastrointestinal tract, responsible for the annual loss of tens of thousands of lives globally. Circular RNA_0075829 (circ_0075829) is known to be dysregulated in various cancers and plays a role in cancer progression. However, its specific function in colon cancer remains largely unexplored. This study aimed to elucidate the function and underlying mechanisms of circ_0075829 in colon cancer through a series of in vitro assays, including cell counting kit-8, flow cytometry, transwell, tube formation, RNA pull-down, dual-luciferase reporter, and western blotting. Additionally, the role of circ_0075829 role in colon cancer was investigated in tumor-bearing mice using immunohistochemistry assays. The findings revealed that circ_0075829 was upregulated in colon cancer and was positively associated with adverse clinical features and poor prognosis in patients. Silencing circ_0075829 resulted in decreased colon cancer cell viability, tube formation, cell invasion, and expression levels of N-cadherin and vascular endothelial growth factor A (VEGFA), while promoting apoptosis and E-cadherin expression. Circ_0075829 acted as a molecular sponge for microRNA-576-3p (miR-576-3p), thereby upregulating the expression of POU class 5 homeobox 1B (POU5F1B) in colon cancer cells. The inhibitory effects of sh-circ_0075829 on the proliferation, invasion, and angiogenesis of colon cancer cells were negated upon miR-576-3p knockdown or POU5F1B overexpression. *In vivo*, experiments demonstrate that circ_0075829 silencing leads to a reduction in tumor size and weight. Furthermore, circ_0075829 knockdown results in increased levels of miR-576-3p and E-cadherin, while decreasing the levels of POU5F1B, N-cadherin, and VEGFA in tumor-bearing mice. Collectively, circ_0075829 promotes proliferation, invasion, and angiogenesis, while inhibiting apoptosis in colon cancer by modulating POU5F1B levels through miR-576-3p sponging.

Keywords: Colon cancer, circ_0075829, miR-576-3p, POU5F1B, angiogenesis

Introduction

Colon cancer, a malignancy of the large intestine or rectum, affects individuals of both genders across various age groups [1]. Its occurrence is attributed to genetic mutations and environmental factors, including age, dietary habits, obesity, smoking, and physical inactivity [1]. Annually, tens of thousands of cases and deaths are reported globally. In the United States, colon cancer is projected to rank third in cancer-related deaths and diagnoses for both sexes in 2024 [2]. Colon cancer is the fourth leading cause of cancer-related mortality in China and is the second most common cancer diagnosis in 2022 [3]. Despite the implementation of various treatment modalities, including colectomy, chemotherapy, radiotherapy, and immunotherapy [4], patients are often diagnosed at an advanced stage when tumor dissemination has already occurred, primarily due to the lack of effective diagnostic strategies. Projections for 2023 indicate that patients with colon cancer face a 20% likelihood of tumor recurrence and distant metastasis, with over 50% of cases developing distant metastasis within five years of initial diagnosis [5]. Consequently, identifying viable targets for the detection and management of colon cancer is of urgent importance.

https://doi.org/10.62347/UHKA5536

Recent studies have highlighted the significant role of circular RNAs (circRNAs) in colon cancer, particularly through their interaction with microRNAs (miRNAs). For example, circHIPK2 sequesters miR-373-3p, thereby inhibiting proliferation and invasion by upregulating the repulsive guidance molecule BMP co-receptor A (RGMA) in colon cancer [6]. Circ_0101050 enhances the expression of maternal embryonic leucine zipper kinase (MELK) by acting as a sponge for miR-140-3p, thereby promoting cell proliferation and tumorigenesis, while also inducing apoptosis in colon cancer cells [7]. Exons 7-8 of the CASC15 gene (chr6:22020567 to 22056919) give rise to circ_0075829, which is upregulated in pancreatic cancer tissues [8-10]. Silencing circ_0075829 inhibits cell proliferation, mobility, and invasion via the miR-1287-5p/lysosomal adaptor, MAPK and MTOR activator 3 (LAMTOR3) axis in pancreatic cancer cells, and reduces tumorigenicity and metastasis in tumor-bearing mice [10]. However, the role and underlying mechanisms of circ_0075829 in colon cancer remain unexplored.

Therefore, this study aims to investigate the potential function and mechanism of circ_0075829 in the progression of colon cancer. We anticipate that our findings will provide a theoretical foundation for the identification and management of colon cancer.

Materials and methods

In silico analysis of circ_0075829 expression in colon cancer

The expression profile of circ_0075829 in colon cancer was analyzed using the GSE142837 microarray dataset, which was obtained from the Gene Expression Omnibus (GEO) database. This dataset comprises five pairs of colorectal cancer tissues and corresponding non-cancerous tissues. The expression profile of POU class 5 homeobox 1B (POU5F1B) in colon cancer was analyzed using the GSE21510, GSE71187, GSE87211 microarray dataset, and TCGA_CRC database. The expression level of circ_0075829 and POU5F1B was assessed utilizing the LIMMA package in the R programming language [11]. Additionally, the relapse-free survival (RFS) of patients with CRC was assessed by the kmplot website (http://kmplot.com/) based on GSE106584 microarray dataset.

Tissue specimen

Colon cancer patients diagnosed and treated at our hospital provided tissue samples, including both cancerous tissues and adjacent normal control tissues (n=66). The normal tissues were collected at a minimum distance of 5 cm from the tumor sites. This study received approval from the Ethics Committee of Renmin Hospital of Wuhan University and was conducted in accordance with the principles outlined in the Declaration of Helsinki. Written informed consent was obtained from all participants.

Reverse transcription quantitative polymerase chain reaction (RT-qPCR)

Total ribonucleic acid (RNA) was extracted from the colon cancer tissues or cells using the TRIzol reagent provided by Sangon Biotech (Shanghai, China; B511311). Subsequently, reverse transcription (RT) assays were performed using the kit from Sangon Biotech (B639252). RT-qPCR was performed using the Bio-Rad CFX Manager software (Bio-Rad Laboratories, Inc., Hercules, CA, USA) in conjunction with the 2×SYBR Green mix (B110031, Sangon Biotech). The expressions levels of circ_0075829 and POU5F1B were quantified employing the $2^{-\Delta\Delta CT}$ method, with glyceraldehyde-3-phosphate dehydrogenase (GAPDH) serving as the reference gene. The Bulge-Loop™ miRNA RT-qPCR Primer (RiboBio Co., Ltd., Guangzhou, China) was utilized to determine the expression of miR-576-3p, using U6 as the internal control. Primer sequences were listed in **Table 1**.

Cell culture

Colon cancer cell lines HCT116 (CL-0096), LOVO (CL-0144), SW480 (CL-0223) and SW620 (CL-0225) were procured from Procell (Wuhan, China), while the human colonic epithelial cell line FHC (CRL-1831) was obtained from the American Type Culture Collection (Manassas, VA). The LOVO, HCT116, SW480, SW620, and FHC cell lines were cultured in McCoy's 5A (PM150710, Procell), Ham's F-12K (PM150910, Procell), Leibovitz's L-15 (PM151010, Procell), Leibovitz's L-15 and DMEM/F12 (PM150312, Procell), respectively, supplemented with 10% fetal bovine serum (FBS, 164210, Procell) at 37°C in a 5% carbon dioxide (CO_2) atmosphere.

Table 1. The primer sequences

Name	Forward (5'-3')	Reverse (5'-3')
circ_0075829	AAGAGAGCCAGCCAGGATCTG	AGAAGGATGTTCAGTAGTAACCCAG
POU5F1B	GTGTTCAGCCAAAAGACCATCT	GGCCTGCATGAGGGTTTCT
GAPDH	GGTGGTCTCCTCTGACTTCAACA	GTTGCTGTAGCCAAATTCGTTGT
miR-576-3p	CGCGAAGATGTGGAAAAATT	AGTGCAGGGTCCGAGGTATT
U6	CTCGCTTCGGCAGCACA	AACGCTTCACGAATTTGCGT

Cell transfection

To modulate the expression levels of circ_0075829, short-hairpin RNAs (shRNAs) specifically targeting circ_0075829 (designated as sh-circ_0075829#1, #2 and #3), along with a scrambled shRNA control (sh-NC), were synthesized and supplied by GenePharma (Shanghai, China). To enhance the expression of miR-576-3p, a miR-576-3p mimic and its corresponding negative control (miR-NC) were also designed and provided by GenePharma. Conversely, to suppress miR-576-3p expression, an anti-miR-576-3p and its respective negative control (anti-NC) were utilized, also sourced from GenePharma. For the upregulation of POU5F1B, its sequences were cloned into pcDNA vector plasmids and transfected into HCT116 cells using Lipofectamine 3000 (L3000001, Invitrogen, Carlsbad, CA, USA).

Cell counting kit-8 (CCK-8) test

HCT116 and SW480 cells were seeded at a density of 5×10^3 cells per well in 96-well plates and incubated in a humidified atmosphere containing 5% CO_2 at 37°C. Subsequently, 10 µl of CCK-8 reagents (CA1210, Solarbio, Beijing, China) was added to each well, and the plates were incubated at 37°C for an additional two hours. Absorbance was measured at 450 nm using a microplate reader from Thermo Fisher Scientific (Waltham, Massachusetts, USA).

Flow cytometry

The apoptosis of HCT116 and SW480 cells was analyzed using flow cytometry with the Annexin V-FITC Apoptosis Detection Kit (CA1020, Solarbio). Transfected HCT116 and SW480 cells were collected and washed with pre-cold phosphate-buffered saline (PBS, E607008, Sangon Biotech). The cells were then resuspended in 1 mL of binding buffer and incubated with the dye for five minutes in the absence of light. Apoptosis rates were evaluated using BD CellQuest Pro software (version 5.1, BD Biosciences, NJ, USA) following examination with a FACScan flow cytometer (BD Biosciences).

Transwell assay

HCT116 and SW480 cells were resuspended in McCoy's 5A medium (for HCT116 cells) or Leibovitz's L-15 medium (for SW480 cells) without FBS and subsequently seeded into the upper chamber of transwell plates at a density of 5×10^4 cells per well. The 24-well transwell plates, featuring an 8-µm pore size and coated with Matrigel (356234, Solarbio), were procured from Corning Company (3422, New York, NY, USA). The lower chamber was supplemented with medium containing 20% FBS. Following a 24-hour incubation period at 37°C in a 5% CO_2 atmosphere, the Matrigel was removed. Cells were fixed using 4% paraformaldehyde (P0099, Beyotime, Shanghai, China) and stained with 0.1% crystal violet (C0121, Beyotime) prior to imaging with an Olympus microscope (Tokyo, Japan). Invasion cells were quantified in five randomly selected fields.

Tube forming experiment

Following the culture of transfected HCT116 and SW480 cells, the supernatant was isolated and incubated with human umbilical vein endothelial cells (HUVECs, C0035C, Gibco, Rockville, MD) under conditions of 5% CO_2 at 37°C. Subsequently, 50 µL of supernatant, containing Matrigel (M8371, Solarbio) diluted in a 1:1 ratio with the supernatant, was dispensed into a 96-well plate. HUVECs at a concentration of 3×10^5 cells/mL were subjected to a 4-hour incubation at 37°C. Imaging was conducted using an Olympus microscope, and tube formation was quantified utilizing ImageJ software (version 2.02, National Institutes of Health, USA).

Dual-luciferase reporter assay

The interaction between circ_0075829 and miR-576-3p was identified using the CircInteractome database platform (https://circinteractome.nia.nih.gov/), while the potential interaction between miR-576-3p and POU5F1B was predicted via the TargetScan database platform (https://www.targetscan.org/vert_80/). To construct luciferase reporter plasmids, wild-type (WT) and mutant (MUT) sequences of circ_0075829 or POU5F1B were cloned into the pGL3-Basic luciferase vector (Promega, Madison, WI, USA). Subsequently, these WT or MUT plasmids were co-transfected into HCT116 or SW480 cells with either miR-NC or miR-576-3p mimic using Lipofectamine 3000. Following a 48-hour transfection period, luciferase activity was measured using the Dual Luciferase Reporter Gene Assay Kit (RG027, Beyotime).

RNA pull-down

The Pierce Magnetic RNA-Protein Pull-Down Kit (Thermo Fisher) was utilized. Biotinylated circ_0075829 probes were incubated with magnetic beads at room temperature for two hours. The mixtures were then incubated with HCT116 or SW480 cells overnight at 4°C. qRT-qPCR was used to detect miR-576-3p following the elution of the magnetic beads.

Fluorescence in situ hybridization (FISH)

The RNA FISH analysis was performed by using the Fluorescence in situ Hybridization Kit (R0306, Beyotime). Transfected HCT116 cells with a density of 1×10^5 cells/well were plated in 12-well plates with cell crawlers (801008, NEST, Wuxi, China). Following 24 h, cells were fixed with 4% paraformaldehyde for 15 min at room temperature. Then, cells were treated based on the operation instruction. The probe (20 μM, 1 μL/well) was denatured for 5 min at 73°C. After hybridization, cells were washed and incubated with Mounting Medium, antifading (with DAPI) (S2110, Solarbio). Images were captured using a fluorescence microscopy (IX71, Olympus, Tokyo, Japan).

Western blotting

To quantify total protein contents, HCT116 and SW480 cells were lysed using radio-immunoprecipitation assay (RIPA) lysis buffer (R0010, Solarbio). Protein concentrations were determined utilizing the BCA Protein Assay Kit (PC0020, Solarbio). Subsequently, protein samples (20 μg) underwent electrophoresis via 10% sodium dodecyl sulfate-polyacrylamide gel electrophoresis (SDS-PAGE) and were transferred onto polyvinylidene fluoride (PVDF) membranes (IPVH00010, Millipore). The membranes were incubated with primary antibodies specific to E-cadherin (1:10000, ab40772, Abcam, Cambridge, UK), N-cadherin (1:1000, ab18203, Abcam), vascular endothelial growth factor A (VEGFA) (1:1000, ab46154, Abcam), POU5F1B (1:1000, ab230429, Abcam), and GAPDH (1:2500, ab9485, Abcam) at 4°C overnight following blocking in a blocking solution (SW-3015, Solarbio) at room temperature for one hour. Subsequently, the membranes were incubated with secondary antibodies (1:10000, ab6721, Abcam) at room temperature for one hour. Bands were visualized using the BeyoECL Plus kit (P0018S, Beyotime), and the gray values were quantified using Image-ProPlus software (Media Cybernetics, Inc., Rockville, MD, USA).

In vivo experiment

Four-week-old BALB/c nude mice were obtained from JK Biot (Nanjing, China) and housed in a specifical pathogen-free (SPF) facility with controlled temperature and a 12-hour light-dark cycle. The mice were randomly assigned to two groups, with six mice each in the sh-circ_0075829 and sh-NC groups. For the subcutaneous injection, HCT116 cell suspension was mixed with Matrigel (211362, NEST) at a ratio of 1:1 at 4°C to prepare a final concentration of 5×10^6 cells/mL, and then 200 μl of the cell mixtures were administered into the right flank of the mice in the sh-circ_0075829 group based on the previous study [12]. In contrast, the sh-NC group received an equivalent number of cell mixtures with sh-NC. Tumor volume was measured weekly for four consecutive weeks using the formula: volume = 0.5 × length × width^2. After five weeks, the mice were euthanized by overexposure to isoflurane (R510-22, RWD, Guangdong, China). Tumor tissues were excised, weighed, and preserved for immunohistochemistry assays. All experimental procedures were approved by the Animal Research Ethics Committee of Renmin Hospital of Wuhan University.

Immunohistochemistry

Following fixation in 4% paraformaldehyde, the tumor tissues underwent dehydration using a graded ethanol series. Subsequently, the tissues were embedded in paraffin (YA0011, Solarbio) and sectioned into 5 μm slices. Antigen retrieval was conducted using a sodium citrate buffer (pH 6.0, P0081, Beyotime) for 15 minutes at 94°C. The sections were then blocked with 1% bovine serum albumin (BSA, ST2249, Beyotime) for one hour. This was followed by an incubation at 4°C for one hour with primary antibodies against POU5F1B (1:100, ab230429, Abcam), E-cadherin (1:100, ab231303, Abcam), N-cadherin (1:100, ab18203, Abcam), and VEGFA (1:50, ab51745, Abcam). The sections were subsequently treated for 30 minutes at 37°C with horseradish peroxidase (HRP)-conjugated anti-rat IgG antibody (ab6734, Abcam) or HRP-conjugated anti-rabbit IgG antibody (ab288151, Abcam). Finally, the sections were stained with hematoxylin (G1080, Solarbio) and visualized using a light microscope (Olympus).

Terminal deoxynucleotidyl transferase deoxyuridine triphosphate (dUTP) nick end labeling (TUNEL) experiments

The paraffin sections were subjected to a 30-minute treatment at room temperature with proteinase K (P9460, Solarbio) following deparaffinization with xylene and dehydration using graded ethanol. Subsequently, the sections were treated with 2% hydrogen peroxide (H_2O_2) for 20 minutes at room temperature after being rinsed three times with PBS. The sections were then incubated for one hour at 37°C with TUNEL reaction mixtures (C1090, Beyotime). Following a 30-minute incubation at room temperature with 500 μL of diaminobenzidine (DAB) (P0202, Beyotime), the sections were further incubated with 50 μL of Streptavidin-HRP (A0305, Beyotime). After counterstaining with hematoxylin (C0107, Beyotime), images were captured using an Olympus light microscope.

Statistical analysis

Data analysis was conducted using IBM SPSS Statistics version 20.0 software (Armonk, New York, USA), and results were expressed as mean ± standard deviation (SD). Statistical differences were assessed using the Student's t-test for two groups or one-way analysis of variance (ANOVA) followed by the *Post Hoc* Bonferroni test among multiple groups. The repeated-measures ANOVA was used for comparisons among multiple groups that include a time variable. Overall survival (OS) was analyzed using the Kaplan-Meier method, with differences assessed via the log-rank test. The relationship between circ_0075829 expression levels and clinicopathological characteristics was examined using the chi-square test. Statistical significance was established at $P<0.05$.

Results

Circ_0075829 was elevated in colon cancer

To investigate the role of circ_0075829 in colon cancer, the expression level of circ_0075829 was initially assessed in colon cancer. As demonstrated in **Figure 1A** and **1B**, the expression level of circ_0075829 was significantly elevated in the colon cancer tissues ($P<0.01$). Patients with colon cancer exhibiting high levels of circ_0075829 had a shorter OS ($P<0.05$, **Figure 1C**), larger tumor sizes ($P=0.024$, **Table 2**), increased lymph node metastasis ($P=0.013$, **Table 2**), and a higher tumor-node-metastasis (TNM) stage ($P=0.046$, **Table 2**) compared to these with low levels of circ_0075829. No statistically significant differences in age ($P=0.618$) and gender ($P=0.447$) were observed between the two groups, as presented in **Table 2**. Additionally, an elevated level of circ_0075829 was detected in colon cancer cell lines, HCT116, LOVO, SW480, and SW620 cells ($P<0.05$, **Figure 1D**). Given the higher levels of circ_0075829 in HCT116 and SW480 cells compared to LOVO and SW620, the former two cell lines were selected for subsequent investigations. Collectively, the increased expression of circ_0075829 was associated with a poor prognosis in colon cancer patients.

Knockdown of circ_0075829 inhibited proliferation, but fostered apoptosis of colon cancer cells

To elucidate the role of circ_0075829 in the progression of colon cancer, three shRNAs targeting circ_0075829 (sh-circ_0075829#1, #2 and #3) were utilized to reduce the circ_0075829 levels in HCT116 and SW480 cells. All three shRNAs effectively decreased the circ_0075829 levels in both cell lines ($P<0.05$,

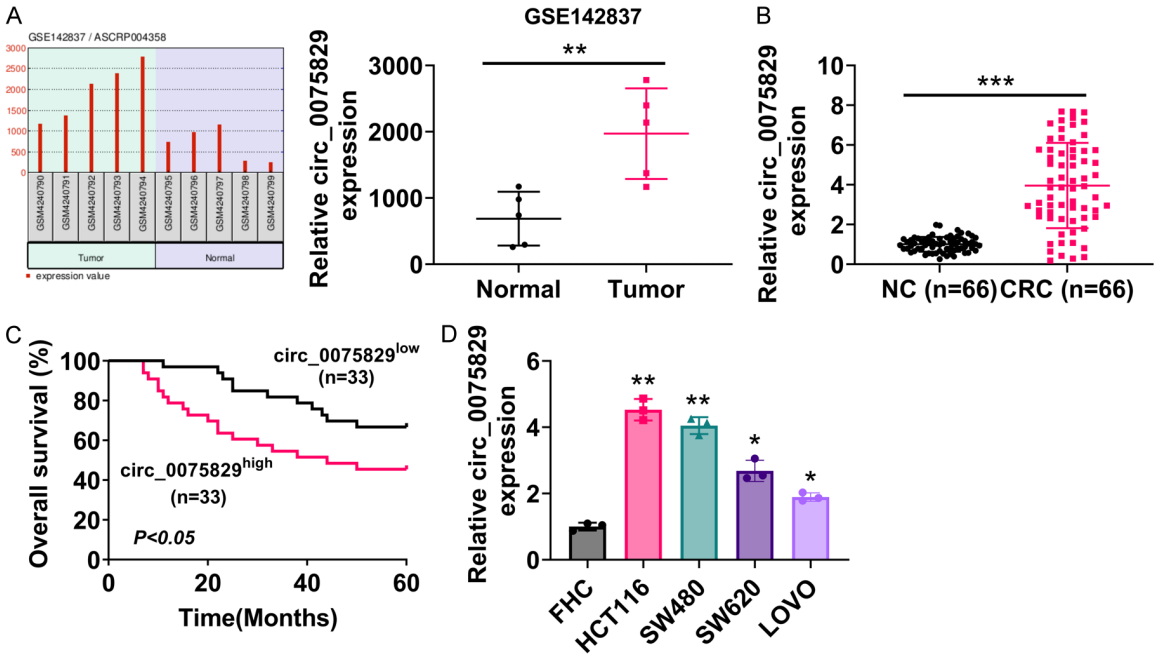

Figure 1. Upregulation of circ_0075829 was associated with poor prognosis in colon cancer patients. (A) The expression level of circ_0075829 in colon tissues was assessed using data from the GSE142837 microarray dataset. **P<0.01. (B) The expression level of *circ_0075829* was measured by RT-qPCR in 66 pairs of colon cancer tissues and adjacent normal control tissues. Data were expressed after being normalized with *GAPDH*. ***P<0.001. (C) A cohort of sixty-six colon cancer patients was stratified into two groups based on circ_0075829 expression levels: a low expression group (n=33) and a high expression group (n=33), using the median circ_0075829 expression value depicted in (B) as the cut-off value. The OS of these groups was analyzed using Kaplan-Meier survival curves. (D) The expression levels of *circ_0075829* were quantified in colon cancer cell lines, namely HCT116, LOVO, SW480, and SW620, using RT-qPCR. Data were expressed after being normalized with *GAPDH*. *P<0.05 and **P<0.01 *vs.* FHC.

Table 2. Correlation between circ_0075829 expression and the clinical pathological features of 66 colon cancer patients

Characteristic	Cases	circ_0075829 expression		*P*-value
		Low (n=33)	High (n=33)	
Age (years)				0.618
<50	28	15	13	
≥50	38	18	20	
Gender				0.447
Female	25	11	14	
Male	41	22	19	
Tumor size				0.024*
<5 cm	39	24	15	
≥5 cm	27	9	18	
Lymph node metastasis				0.013*
Yes	36	13	23	
No	30	20	10	
TNM				0.046*
I+II	38	23	15	
III	28	10	18	

Note: A chi-square test was used for comparing groups between low and high circ_0075829 expression. *P<0.05.

Figure 2A), with sh-circ_0075829#3 demonstrating superior interference efficiency compared to sh-circ_0075829#1 and #2. Consequently, sh-circ_0075829#3 was selected for subsequent assays and referred to as sh-circ_0075829. No significant difference in circ_0075829 expression was found between the sh-NC group and the control group (without treatment) (P>0.05, **Figure 2A**). The transfection of sh-circ_0075829 resulted in a significant decrease in cell viability while simultaneously increasing the apoptosis rate in both cell lines (P<0.01, **Figure 2B-D**). Totally, the silencing of circ_0075829 inhibited proliferation and promoted apoptosis in colon cancer cells.

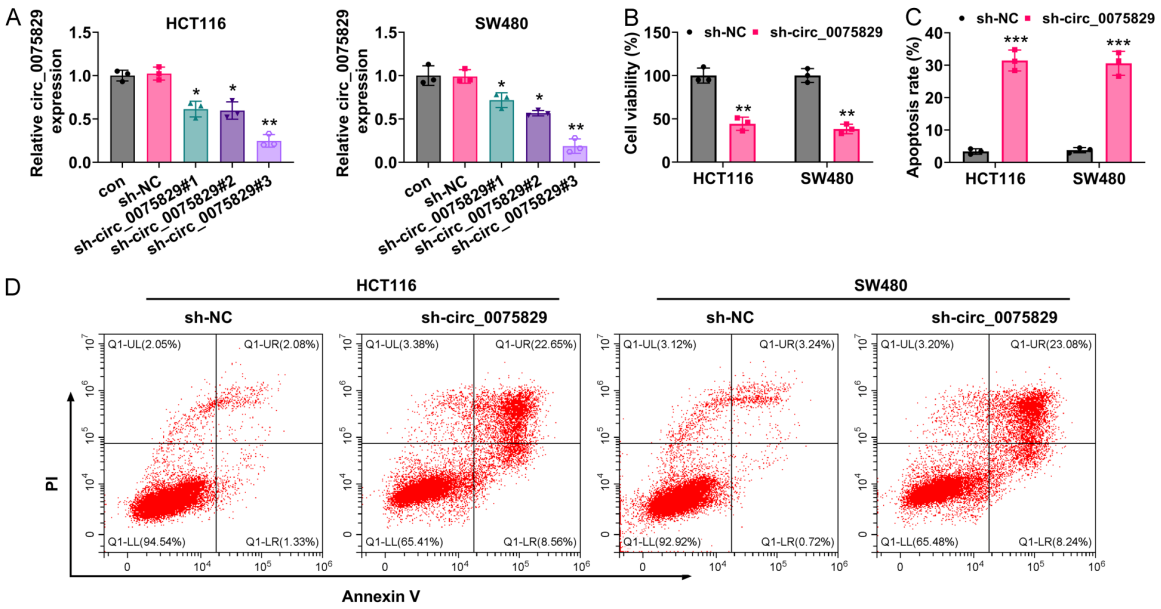

Figure 2. Interference with circ_0075829 suppressed proliferation, and increased apoptosis in colon cancer cells. A. The efficiency of three shRNAs targeting circ_0075829 was evaluated via RT-qPCR. Data were expressed after being normalized with *GAPDH*. B. Cell viability of HCT116 and SW480 was assessed using CCK-8 assays. C and D. Apoptosis rates in HCT116 and SW480 cells were measured by flow cytometry. *P<0.05, **P<0.01 and ***<0.001 *vs.* sh-NC.

Downregulation of circ_0075829 impaired the invasion and angiogenesis capabilities of colon cancer cells

Specifically, interference with circ_0075829 led to a reduction in the number of invaded cells and the level of N-cadherin, while increasing the level of E-cadherin in HCT116 and SW480 cells (P<0.01, **Figure 3A** and **3C**). Additionally, silencing circ_0075829 decreased the relative tube formation of HUVECs and reduced VEGFA expression in both cell lines (P<0.01, **Figure 3B** and **3C**). Altogether, these findings indicate that the silencing of circ_0075829 suppressed the invasion and angiogenesis of colon cancer cells.

Circ_0075829 targeted miR-576-3p

Considering that circRNAs typically function as competing endogenouse RNAs (ceRNAs) by acting as molecular sponges for miRNA, potential miRNAs interactions were predicted using the CircInteractome online platform. Complementary base pairings were identified between circ_0075829 and miR-576-3p (**Figure 4A**). To validate the interaction between circ_0075829 and miR-576-3p, miR-576-3p expression was upregulated in HCT116 and SW480 cells through transfection with miR-576-3p mimics (P<0.001, **Figure 4B**). Co-transfection with miR-576-3p mimics and circ_0075829-WT, but not circ_0075829-MUT, resulted in a significant decrease in relative luciferase activity in both cell lines (P<0.01, **Figure 4C**), suggesting a direct binding between circ_0075829 and miR-576-3p. Furthermore, RNA pull-down assays demonstrated that biotinylated circ_0075829 probes enriched miR-576-3p more effectively than NC probes in both cell lines (P<0.001, **Figure 4D**). In addition, FISH results demonstrated that miR-576-3p was expressed on the cytoplasm, and knockdown of circ_0075829 had no effect on the subcellular localization of miR-576-3p (Supplementary Figure 1). Collectively, these findings indicate that circ_0075829 directly targeted miR-576-3p.

Circ_0075829 positively regulated the protein level of POU5F1B by targeting miR-576-3p

Complementary base pairings between miR-576-3p and POU5F1B were identified (**Figure 5A**). Consistently, dual-luciferase reporter assays confirmed the direct interaction between miR-576-3p and POU5F1B (P<0.01, **Figure 5B** and **5C**). Upregulation of miR-576-3p led to a reduction in POU5F1B levels in both HCT116 and SW480 cells (P<0.01, **Figure 5D**), indicating an anticipated negative correlation between

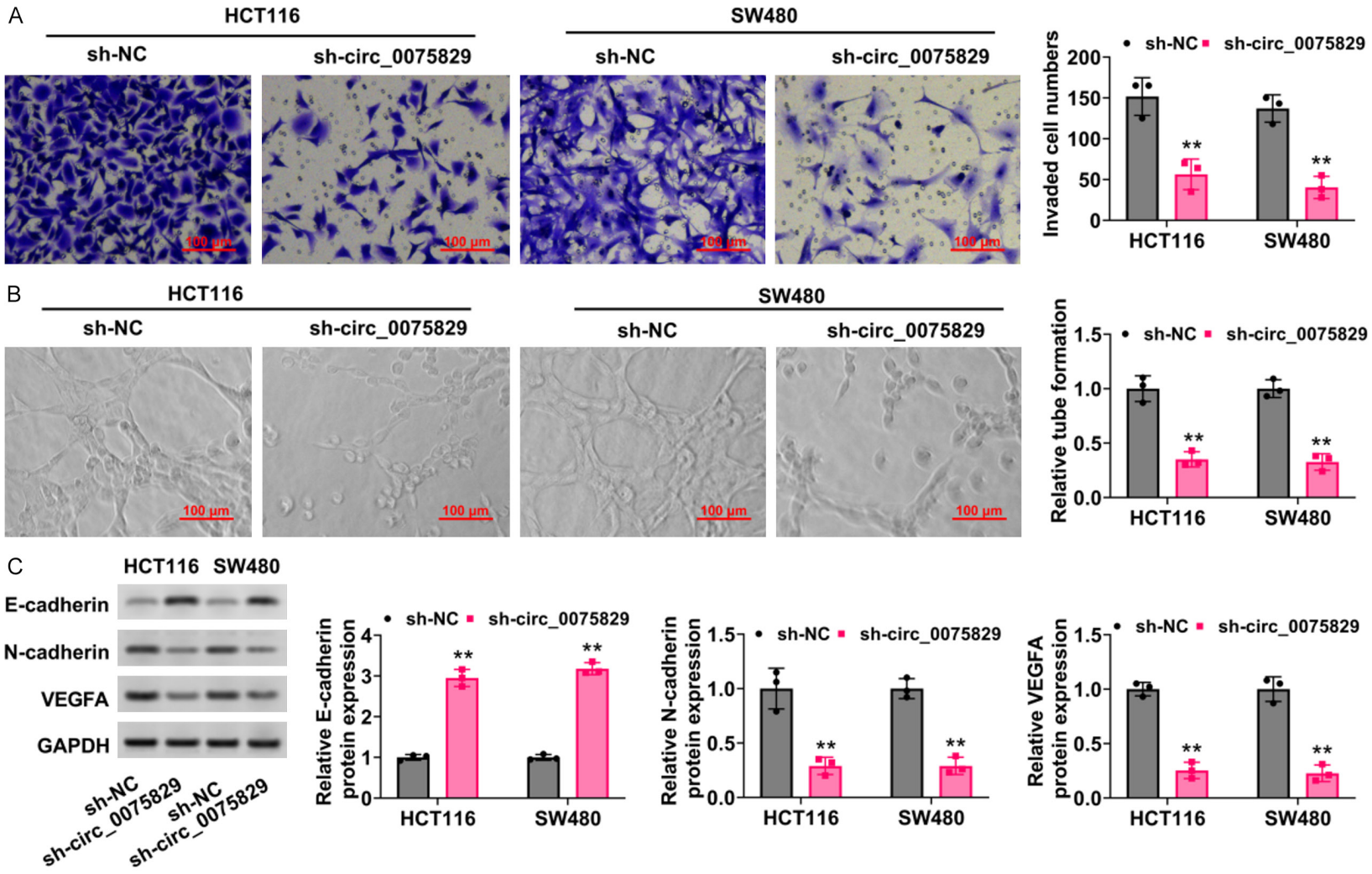

Figure 3. Downregulation of circ_0075829 impaired the invasion and angiogenesis capabilities of colon cancer cells. A. The invasive potential of HCT116 and SW480 cells was evaluated using transwell assays. Magnification: ×200, Scale bar =100 μm. B. Tube formation by HUVECs was assessed through tube formation assays. Magnification: ×200, Scale bar =100 μm. C. The relative protein expression levels of E-cadherin, N-cadherin, and VEGFA were assessed via western blot analysis. Data were expressed after being normalized with GAPDH. **P<0.01 *vs.* sh-NC.

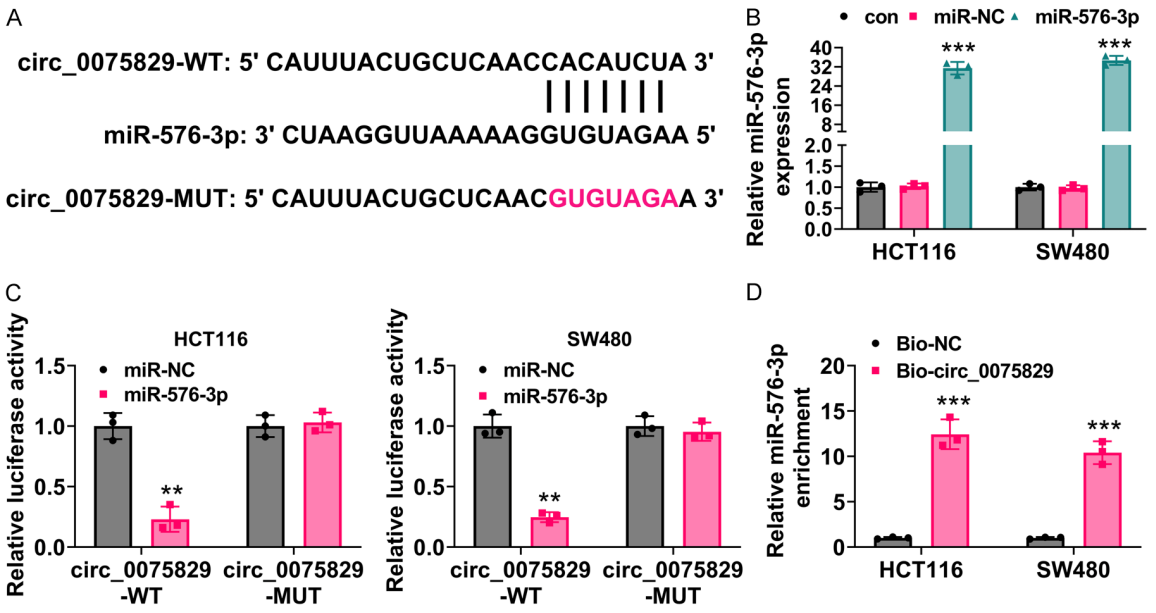

Figure 4. Circ_0075829 directly targeted miR-576-3p. A. The binding sites between circ_0075829 and miR-576-3p were predicted through the CircInteractome online platform, along with the design and presentation of both wild-type and mutant sequences of circ_0075829. B. The overexpression efficiency of miR-576-3p was measured by qRT-PCR. The data were normalized with *U6*. ***P<0.001 *vs.* miR-NC. C. The luciferase activity was determined in HCT116 and SW480 cells by the Dual Luciferase Reporter Assay System. **P<0.01 *vs.* miR-NC. D. RNA pull-down assays showed enrichment of miR-576-3p using biotinylated circ_0075829 probes. ***P<0.001 *vs.* Bio-NC.

miR-576-3p and POU5F1B. To further validate the interaction among circ_0075829, miR-576-3p, and POU5F1B, the level of miR-576-3p was reduced through the administration of anti-miR-576-3p (P<0.01, **Figure 5E**). The silencing of circ_0075829 led to a decrease in POU5F1B expression in both cell lines, which was subsequently restored by treatment with anti-miR-576-3p (P<0.01, **Figure 5F**). In addition, the expression level of POU5F1B was significantly elevated in the colon cancer tissues based on the GSE21510, GSE71187, GSE87211 microarray dataset, and TCGA_CRC databases (P< 0.001, Supplementary Figure 2A). Patients with colon cancer exhibiting high levels of POU5F1B had a shorter RFS based on the GSE106584 microarray dataset (P<0.001, Supplementary Figure 2B). Altogether, circ_0075829 was found to positively regulate the protein expression of POU5F1B by targeting miR-576-3p.

Circ_0075829 facilitated the growth, invasion, and angiogenesis of colon cancer cells while inhibiting apoptosis through the miR-576-3p/POU5F1B pathway

To investigate the role of circ_0075829 in the progressions of colon cancer via the miR-576-3p/POU5F1B axis, POU5F1B expression was upregulated in HCT116 cells (P<0.01, **Figure 6A**). The transfection of sh-circ_0075829 into HCT116 cells resulted in decreased cell viability and increased apoptosis rates, effects that were reversed by the silencing of miR-576-3p (P<0.05) or the overexpression of POU5F1B (P<0.01) (**Figure 6B-D**). Furthermore, the downregulation of miR-576-3p or the overexpression of POU5F1B restored the number of invaded cells and the relative tube formation in HCT116 cells with sh-circ_0075829 (P<0.05, **Figure 7A** and **7B**). Overall, circ_0075829 was found to promote colon cancer cell proliferation, invasion, and angiogenesis while inhibiting apoptosis via the miR-576-3p/POU5F1B pathway.

Knockdown circ_0075829 suppressed colon cancer cell proliferation, invasion and angiogenesis, but enhanced apoptosis in vivo

The role of circ_0075829 was further investigated *in vivo*, where mice were subcutaneously injected with HCT116 cells expressing circ_0075829. Mice treated with sh-circ_0075829 exhibited significantly smaller tumor sizes and reduced tumor weights compared to those treated with sh-NC (P<0.01), although there was no statistically significant difference in

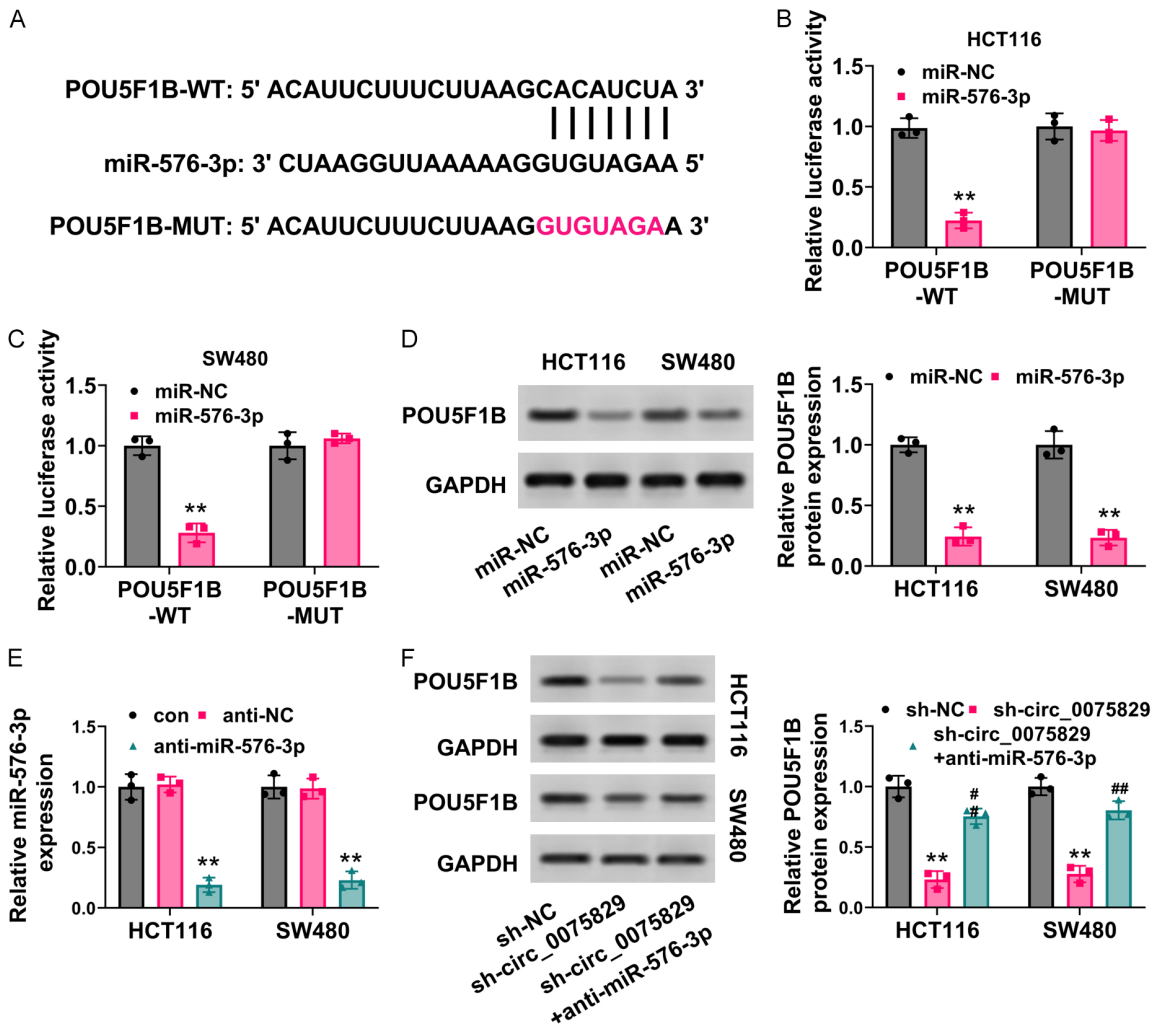

Figure 5. Circ_0075829 positively regulated the protein expression of POU5F1B by targeting miR-576-3p. A. The binding sites between miR-576-3p and POU5F1B were predicted by the TargetScan online platform, along with the design and presentation of both wild-type and mutant sequences of POU5F1B. B. The luciferase activity was determined in HCT116 cells using the Dual Luciferase Reporter Assay System. **P<0.01 *vs.* miR-NC. C. The luciferase activity was determined in SW480 cells using the Dual Luciferase Reporter Assay System. **P<0.01 *vs.* miR-NC. D. The relative protein expression of POU5F1B was assessed using western blot analysis following the transfection of HCT116 and SW480 cells with either miR-576-3p mimics or miR-NC. Data were normalized with GAPDH. E. The knockdown efficiency of miR-576-3p was evaluated through qRT-PCR. The data were normalized with *U6*. **P<0.01 *vs.* anti-NC. F. The relative protein expression of POU5F1B was determined via western blot. Data were normalized with GAPDH. **P<0.01 *vs.* sh-NC; ##P<0.01 *vs.* sh-circ_0075829.

overall body weight between the two groups (**Figure 8A-C**). The knockdown of circ_0075829 resulted in decreased transcriptional expression of POU5F1B and increased levels of miR-576-3p in tumor samples (P<0.01, **Figure 8D**). Furthermore, silencing circ_0075829 led to a significant increase in the apoptosis rate (P< 0.01, **Figure 8E** and **8G**). Meanwhile, the downregulation of circ_0075829 in tumor tissues resulted in reduced protein levels of POU5F1B, N-cadherin, and VEGFA, while E-cadherin expression was upregulated (P<0.01, **Figure 8F** and **8G**). Collectively, these findings indicate that silencing circ_0075829 suppressed colon cancer cell growth, invasion, and angiogenesis, while promoting apoptosis through the miR-576-3p/POU5F1B axis in xenografted mice. In summary, the findings of this study indicated that circ_0075829 promoted the proliferation, invasion, and angiogenesis of colon cancer cells while inhibiting apoptosis through the miR-576-3p/POU5F1B axis (see **Figure 9**).

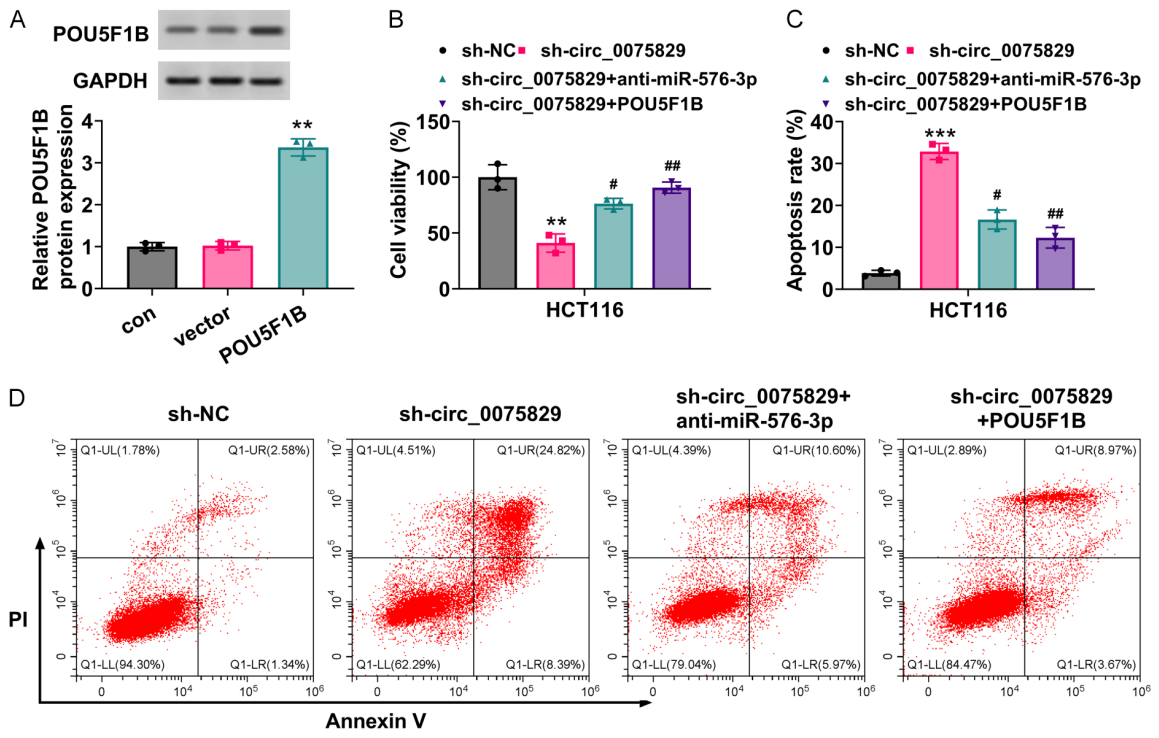

Figure 6. Circ_0075829 promoted proliferation and reduced apoptosis in colon cancer cells through the miR-576-3p/POU5F1B pathway. A. The overexpression efficiency of POU5F1B was verified by western blot. The data were normalized with GAPDH. **P<0.01 *vs.* vector. B. HCT116 cell viability was assessed using CCK-8 assays. **P<0.01 *vs.* sh-NC; #P<0.05 and ##P<0.01 *vs.* sh-circ_0075829. C and D. HCT116 cell apoptosis rates were determined by flow cytometry. ***P<0.001 *vs.* sh-NC; #P<0.05 and ##P<0.01 *vs.* sh-circ_0075829.

Discussion

Colon cancer, a malignancy of the large intestine or rectum, is characterized by high invasiveness and ranks among the most prevalent and lethal cancers globally [13]. The disease is marked by nonspecific early symptoms, posing significant challenges to diagnosis and treatment. Therefore, the identification of potential targets is crucial for the effective detection and management of colon cancer. The research revealed that circ_0075829 expression was upregulated in colon cancer, correlating with a poor prognosis for patients. Silencing circ_0075829 resulted in reduced proliferation, invasion, and angiogenesis, alongside increased apoptosis in colon cancer cells. Mechanistically, circ_0075829 acted as a molecular sponge for miR-576-3p, thereby upregulating POU5F1B expression in colon cancer cells. The suppressive effects of sh-circ_0075829 on proliferation, invasion, and angiogenesis, as well as its pro-apoptotic influence, were negated by either miR-576-3p knockdown or POU5F1B overexpression. *In vivo* experiments demonstrated that circ_0075829 silencing led to decreased tumor volume and weight, along with reduced levels of POU5F1B, N-cadherin, and VEGFA, while increasing miR-576-3p and E-cadherin levels, as well as apoptosis rates. Taken together, these results underscore the role of circ_0075829 in enhancing growth, invasion, and angiogenesis, and in suppressing apoptosis of colon cancer cells via the miR-576-3p/POU5F1B axis.

The dysregulation of various circRNAs in colon cancer suggests their potential as targets for the identification and management of this malignancy [14]. The current study focuses on circ_0075829, which has been shown to be highly expressed in pancreatic cancer tissues [8-10], and cell lines [10], with a negative correlation to regional lymphatic metastasis and tumor size in pancreatic cancer patients [10]. In this study, circ_0075829 was found to be elevated in colon cancer tissues and cells, and its expression was associated with shorter OS, increased lymph node metastasis, and a higher TNM stage in colon cancer patients. These find-

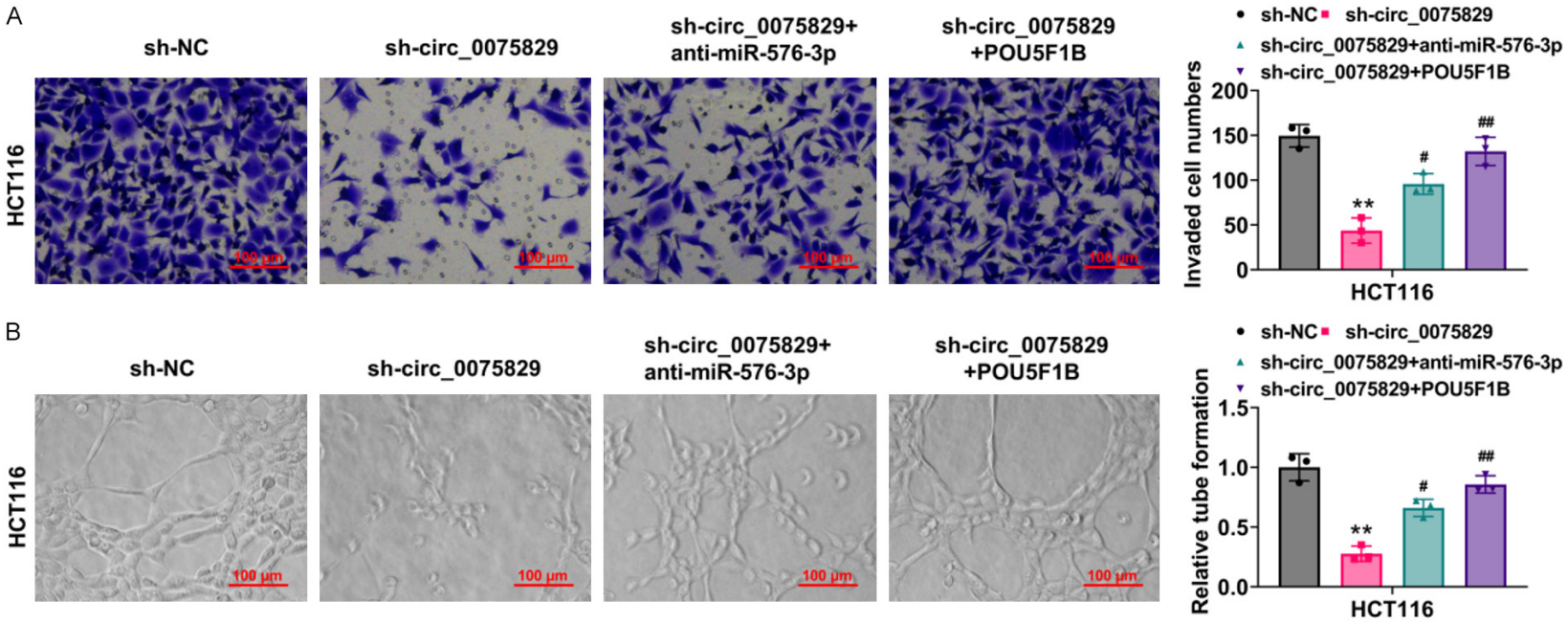

Figure 7. Circ_0075829 enhanced the invasion and angiogenesis of colon cancer cells via the miR-576-3p/POU5F1B pathway. A. The invasive capacity of HCT116 cells was evaluated using transwell assays. Magnification: ×200, Scale bar =100 μm. B. The relative tube formation of HCT116 cells was assessed through by tube formation assays. Magnification: ×200, Scale bar =100 μm. **P<0.01 *vs.* sh-NC; #P<0.05 and ##P<0.01 *vs.* sh-circ_0075829.

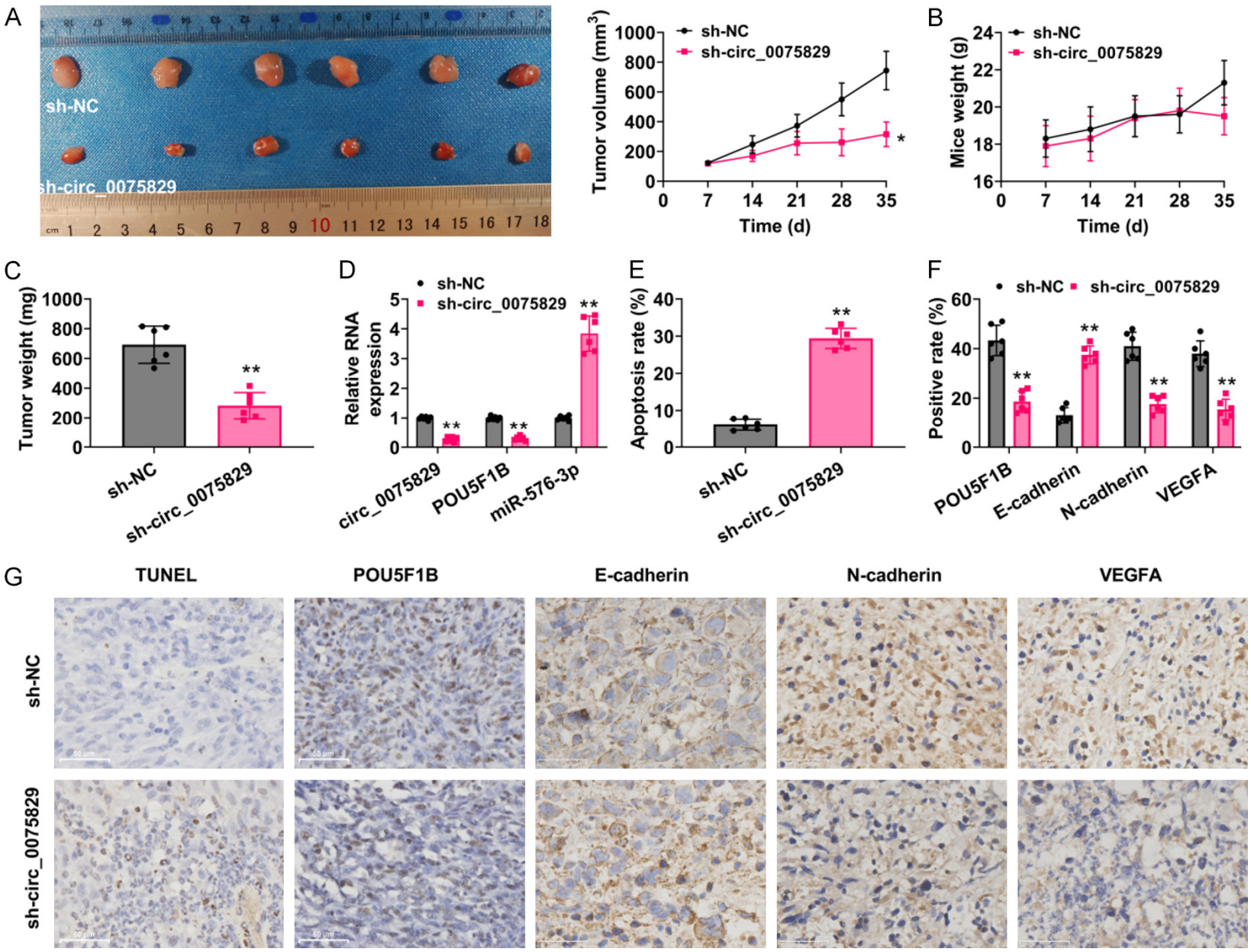
A
sh-NC
sh-circ_0075829
Tumor volume (mm3)
Time (d)
B
Mice weight (g)
Time (d)
C
Tumor weight (mg)
D
Relative RNA expression
circ_0075829
POU5F1B
miR-576-3p
E
Apoptosis rate (%)
F
Positive rate (%)
POU5F1B
E-cadherin
N-cadherin
VEGFA
G
TUNEL
POU5F1B
E-cadherin
N-cadherin
VEGFA

Figure 8. Knockdown of circ_0075829 inhibited colon cancer cell growth, invasion, and angiogenesis, while enhancing apoptosis involved in the miR-576-3p/POU5F1B axis in xenografted mice. HCT116 cell suspension was mixed with Matrigel at a ratio of 1:1 at 4°C to prepare a final concentration of 5×10^6 cells/mL, and then 200 μl of the cell mixtures were administered into the right flank of the nude mice. A. Representative images of neoplasms from nude mice (Left), alongside weekly monitoring of tumor volume over a four-week period (Right). Tumor volume was calculated using the formula: volume = 0.5 × length × width^2. B. Body weight of the mice was monitored weekly for four consecutive weeks. C. Tumor weight was measured after five weeks. D. The expression levels of *circ_0075829*, *POU5F1B*, and *miR-576-3p* in tumor tissues were analyzed via RT-qPCR in tumor tissues. Data were expressed after being normalized with *GAPDH* or *U6*. E. The apoptosis rate was assessed using TUNEL assays. F. The relative expression levels of POU5F1B, E-cadherin, N-cadherin, and VEGFA were quantified through immunohistochemical analysis. G. Apoptosis was evaluated by TUNEL staining, and the expression levels of POU5F1B, E-cadherin, N-cadherin, and VEGFA were determined by immunohistochemistry. Magnification: ×400, Scale bar =50 μm. **P<0.01 *vs.* sh-NC.

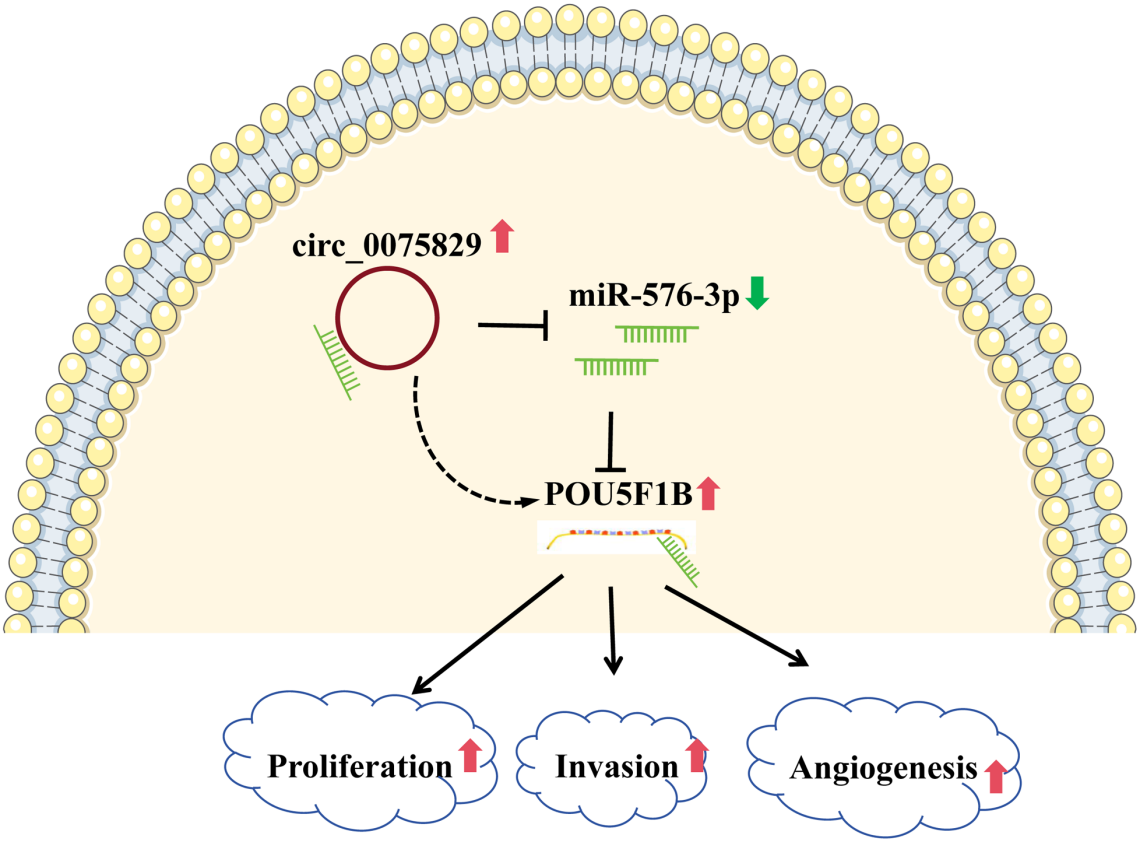

Figure 9. Graphical Abstract illustrating circ_0075829 promotes colon cancer. circ_0075829 was significantly elevated in the colon cancer tissues. circ_0075829 promoted the proliferation, invasion and angiogenesis of colon cancer cells through the miR-576-3p/POU5F1B axis.

ings suggested that the upregulation of circ_0075829 was indicative of a poor prognosis in colon cancer patients.

The dysregulation of circ_0075829 in colon cancer suggested that circ_0075829 might play a role in the progression and development of the disease. In this study, the knockdown of circ_0075829 was found to decrease the viability of colon cancer cells while increasing the apoptosis rate in HCT116 and SW480 cell lines. Furthermore, the knockdown of circ_0075829 resulted in reduced tumor size and weight, alongside an increase in TUNEL-positive staining rates in tumor tissues derived from xenografted mice with HCT116 cells. These findings indicated that the silencing of circ_0075829 inhibited colon cancer cell growth, and promoted apoptosis both *in vitro* and *in vivo*. Additionally, the silencing of circ_0075829 led to a reduction in the number of invaded cells in colon cancer cell lines. The knockdown also

resulted in a decreased level of N-cadherin and an increased level of E-cadherin level in both cell and animal models of colon cancer. Epithelial-mesenchymal transition (EMT) plays a critical role in promoting metastasis across various malignancies [6, 7], characterized by a decreased level of E-cadherin and increased levels of N-cadherin and Vimentin, which are key features of this process [15, 16]. EMT is closely associated with cancer invasion [17]. These findings demonstrated that the silencing of circ_0075829 suppressed the invasion of colon cancer cells. Furthermore, the downregulation of circ_0075829 decreased the relative tube formation of HUVECs *in vitro* and reduced VEGFA expression both *in vitro* and *in vivo*. VEGFA is a critical mediator of angiogenesis, whose activation can facilitate tumor growth [18]. The capacities for proliferation, apoptosis, invasion, and angiogenesis are fundamental and prominent characteristics of cancers, including colon cancer [19]. CircRNAs influence various aspects of colon cancer, such as growth, invasion, apoptosis, migration, and drug resistance [14]. Additionally, the knockdown of circ_0075829 inhibited the growth, mobility, and invasion of pancreatic cancer cells through the miR-1287-5p/LAMTOR3 axis and reduced tumorigenicity and metastasis in tumor-bearing mice with pancreatic cancer cells [10]. The downregulation of circ_0075829 also hindered proliferation, invasion, migration, and glutamine metabolism, while enhancing cell apoptosis and gemcitabine (GEM) sensitivity in GEM-resistant pancreatic cancer cells via the miR-326/GOT1 axis [20]. Overall, the downregulation of circ_0075829 suppressed growth, invasion, and angiogenesis, while inducing apoptosis in colon cancer cells.

The most notable feature of circRNAs is their function as molecular sponges for miRNA via the ceRNA mechanism, thereby modulating gene expression [21]. A growing body of evidence indicates that circRNAs play a regulatory role in the progression and development of colon cancer through the ceRNA mechanism. For instance, Li et al. [22] demonstrated that hsa_circ_0104206 acted as a sponge for miR-188-3p, influencing the levels of cyclin A2 (CCNA2) level and thereby promoting the proliferation and migration of colon cancer cell. Similarly, hsa_circ_0008234 enhanced the proliferation, invasion, and metastasis of colon cancer cells through the miR-338-3p/ETS1 pathway [23]. In this study, miR-576-3p was identified as a target of circ_0075829, with their direct interaction confirmed via luciferase reporter and pull-down assays. Notably, miR-576-3p is found to be downregulated in colon cancer tissues [24]. Furthermore, miR-576-3p is also sequestered by circRNAs to regulate target gene expression, thereby influencing cancer progression and development. For instance, hsa_circ_0012673 sponges miR-576-3p to modulate the expression of SRY-box transcription factor 4 (SOX4), facilitating the growth, mobility, and invasion of breast cancer cells [25]. In gastric cancer, circDNMT1 facilitated malignant progression through the miR-576-3p/hypoxia inducible factor-1 alpha (HIF-1α) pathway [26]. Further investigation revealed that miR-576-3p can directly interact with POU5F1B in this study. POU5F1B, located on chromosomal band 8q24, encodes a protein with 95% sequence homology to octamer-binding transcription factor 4 (OCT4A), which is known to be dysregulated in various cancers and influences multiple downstream pathways. For instance, POU5F1B is highly expressed in gastric cancer cell lines and clinical specimens, where its overexpression results in proliferative, mitogenic, aggressive, angiogenic, and anti-apoptotic effects in gastric cancer xenografts [27]. Additionally, POU5F1B was is upregulated in hepatocellular carcinoma cells and tissues, promoting proliferation via activation of protein kinase B (AKT) [28]. In cervical cancer tissues and cell lines, POU5F1B is markedly upregulated, and its expression interference significantly inhibits cell proliferation, migration, and invasion, while inducing apoptosis [29]. Elevated expression of POU5F1B enhances the proliferation and metastatic potential of colorectal cancer cells [30]. In colon cancer, POU5F1B expression is upregulated and is significantly associated with poor clinical prognosis in patients [31]. Furthermore, POU5F1B promotes the growth and metastasis of colon cancer cells [30]. In the present study, knockdown of circ_0075829 reduced the relative protein expression of POU5F1B in colon cancer cells, an effect that was reversed by the administration of anti-miR-576-3p. Collectively, these findings suggested that circ_0075829 positively regulated the protein expression of POU5F1B by targeting miR-576-3p.

Conclusion

In summary, our data further elucidated that the upregulation of circ_0075829 was a marker of poor prognosis in colon cancer. The knockdown of circ_0075829 inhibited cell growth, invasion, and angiogenesis, while promoting apoptosis in colon cancer cells. Mechanistically, circ_0075829 acted as a sponge for miR-576-3p, thereby modulating the expression of POU5F1B and influencing the progression of colon cancer. However, several limitations need to be addressed in future research. For instance, future studies should investigate the role of circ_0075829 in the migration, stemness, and resistance of colon cancer. Furthermore, it is imperative to investigate the direct effects of the circ_0075829/miR-576-3p/POU5F1B axis through *in vivo* experiments. In summary, these findings present a potential target for the clinical diagnosis and treatment of colon cancer.

Disclosure of conflict of interest

None.

Address correspondence to: Yongbin Zheng, Department of Gastrointestinal Surgery, Renmin Hospital of Wuhan University, 238 Jiefang Street, Wuchang, Wuhan 430060, Hubei, P. R. China. E-mail: whuzhengyongbin@21cn.com

References

[1] Dekker E, Tanis PJ, Vleugels JLA, Kasi PM and Wallace MB. Colorectal cancer. Lancet 2019; 394: 1467-1480.
[2] Siegel RL, Giaquinto AN and Jemal A. Cancer statistics, 2024. CA Cancer J Clin 2024; 74: 12-49.
[3] Han B, Zheng R, Zeng H, Wang S, Sun K, Chen R, Li L, Wei W and He J. Cancer incidence and mortality in China, 2022. J Natl Cancer Cent 2024; 4: 47-53.
[4] Miller KD, Nogueira L, Devasia T, Mariotto AB, Yabroff KR, Jemal A, Kramer J and Siegel RL. Cancer treatment and survivorship statistics, 2022. CA Cancer J Clin 2022; 72: 409-436.
[5] Siegel RL, Wagle NS, Cercek A, Smith RA and Jemal A. Colorectal cancer statistics, 2023. CA Cancer J Clin 2023; 73: 233-254.
[6] Lun J, Zhang Y, Yu M, Zhai W, Zhu L, Liu H, Guo J, Zhang G, Qiu W and Fang J. Circular RNA circHIPK2 inhibits colon cancer cells through miR-373-3p/RGMA axis. Cancer Lett 2024; 216957.
[7] Cheng K, Chen H, Chen B, Li J, Fan C, Yan H, Huang W, Zhao T, Luo Y and Peng L. Hsa_circ_0101050 accelerates the progression of Colon cancer by targeting the miR-140-3 p/MELK axis. Transl Oncol 2024; 44: 101890.
[8] Yang J, Cong X, Ren M, Sun H, Liu T, Chen G, Wang Q, Li Z, Yu S and Yang Q. Circular RNA hsa_circRNA_0007334 is predicted to promote MMP7 and COL1A1 expression by functioning as a miRNA sponge in pancreatic ductal adenocarcinoma. J Oncol 2019; 2019: 7630894.
[9] Zhang Q, Wang JY, Zhou SY, Yang SJ and Zhong SL. Circular RNA expression in pancreatic ductal adenocarcinoma. Oncol Lett 2019; 18: 2923-2930.
[10] Zhang X, Xue C, Cui X, Zhou Z, Fu Y, Yin X, Wu S, Gong Y, Liu Y, Zhu C and Qin X. Circ_0075829 facilitates the progression of pancreatic carcinoma by sponging miR-1287-5p and activating LAMTOR3 signalling. J Cell Mol Med 2020; 24: 14596-14607.
[11] Smyth GK. Linear models and empirical bayes methods for assessing differential expression in microarray experiments. Stat Appl Genet Mol Biol 2004; 3: Article3.
[12] Wang J, Zhang Y, Song H, Yin H, Jiang T, Xu Y, Liu L, Wang H, Gao H, Wang R and Song J. The circular RNA circSPARC enhances the migration and proliferation of colorectal cancer by regulating the JAK/STAT pathway. Mol Cancer 2021; 20: 81.
[13] Bray F, Laversanne M, Sung H, Ferlay J, Siegel RL, Soerjomataram I and Jemal A. Global cancer statistics 2022: GLOBOCAN estimates of incidence and mortality worldwide for 36 cancers in 185 countries. CA Cancer J Clin 2024; 74: 229-263.
[14] Huang J, Yu S, Ding L, Ma L, Chen H, Zhou H, Zou Y, Yu M, Lin J and Cui Q. The dual role of circular RNAs as miRNA sponges in breast cancer and colon cancer. Biomedicines 2021; 9: 1590.
[15] Bracken CP and Goodall GJ. The many regulators of epithelial-mesenchymal transition. Nat Rev Mol Cell Biol 2022; 23: 89-90.
[16] Dongre A and Weinberg RA. New insights into the mechanisms of epithelial-mesenchymal transition and implications for cancer. Nat Rev Mol Cell Biol 2019; 20: 69-84.
[17] Das V, Bhattacharya S, Chikkaputtaiah C, Hazra S and Pal M. The basics of epithelial-mesenchymal transition (EMT): a study from a structure, dynamics, and functional perspective. J Cell Physiol 2019; 234: 14535-14555.
[18] Kang Y, Li H, Liu Y and Li Z. Regulation of VEGF-A expression and VEGF-A-targeted therapy in malignant tumors. J Cancer Res Clin Oncol 2024; 150: 221.

[19] Hanahan D. Hallmarks of cancer: new dimensions. Cancer Discov 2022; 12: 31-46.
[20] Xiang Y, Zhou R, Yang Y, Bai H, Liang F, Wang H and Wang X. A Novel circ_0075829/miR-326/GOT1 ceRNA crosstalk regulates the malignant phenotypes and drug sensitivity of gemcitabine-resistant pancreatic cancer cells. J Biochem Mol Toxicol 2025; 39: e70089.
[21] Panda AC. Circular RNAs act as miRNA sponges. Adv Exp Med Biol 2018; 1087: 67-79.
[22] Li Z, Li Q and Chen Z. Hsa_Circ_0104206 is an oncogenic circRNA in colon cancer by targeting Mir-188-3p/CCNA2 axis. Horm Metab Res 2023; 55: 498-505.
[23] Wu D, Li Y, Xu A, Tang W and Yu B. CircRNA RNA hsa_circ_0008234 promotes colon cancer progression by regulating the miR-338-3p/ETS1 axis and PI3K/AKT/mTOR signaling. Cancers (Basel) 2023; 15: 2068.
[24] Eldaly MN, Metwally FM, Shousha WG, El-Saiid AS and Ramadan SS. Clinical potentials of miR-576-3p, miR-613, NDRG2 and YKL40 in colorectal cancer patients. Asian Pac J Cancer Prev 2020; 21: 1689-1695.
[25] Qiu X, Zhang Q, Deng Q and Li Q. Circular RNA hsa_circ_0012673 promotes breast cancer progression via miR-576-3p/SOX4 axis. Mol Biotechnol 2023; 65: 61-71.
[26] Li H, Cao B, Zhao R, Li T, Xu X, Cui H, Deng H, Gao J and Wei B. circDNMT1 promotes malignant progression of gastric cancer through targeting miR-576-3p/hypoxia inducible factor-1 Alpha axis. Front Oncol 2022; 12: 817192.
[27] Hayashi H, Arao T, Togashi Y, Kato H, Fujita Y, De Velasco MA, Kimura H, Matsumoto K, Tanaka K, Okamoto I, Ito A, Yamada Y, Nakagawa K and Nishio K. The OCT4 pseudogene POU5F1B is amplified and promotes an aggressive phenotype in gastric cancer. Oncogene 2015; 34: 199-208.
[28] Pan Y, Zhan L, Chen L, Zhang H, Sun C and Xing C. POU5F1B promotes hepatocellular carcinoma proliferation by activating AKT. Biomed Pharmacother 2018; 100: 374-380.
[29] Yu J, Zhang J, Zhou L, Li H, Deng ZQ and Meng B. The Octamer-Binding Transcription Factor 4 (OCT4) pseudogene, POU domain class 5 transcription factor 1B (POU5F1B), is upregulated in cervical cancer and down-regulation inhibits cell proliferation and migration and induces apoptosis in cervical cancer cell lines. Med Sci Monit 2019; 25: 1204-1213.
[30] Simó-Riudalbas L, Offner S, Planet E, Duc J, Abrami L, Dind S, Coudray A, Coto-Llerena M, Ercan C, Piscuoglio S, Andersen CL, Bramsen JB and Trono D. Transposon-activated POU5F1B promotes colorectal cancer growth and metastasis. Nat Commun 2022; 13: 4913.
[31] Tao HC, Wang C, Ma N, Zhu X and Zhou XJ. Recurrent superenhancer of the oncogene POU5F1B in colorectal cancers. Biomed Res Int 2021; 2021: 5405060.

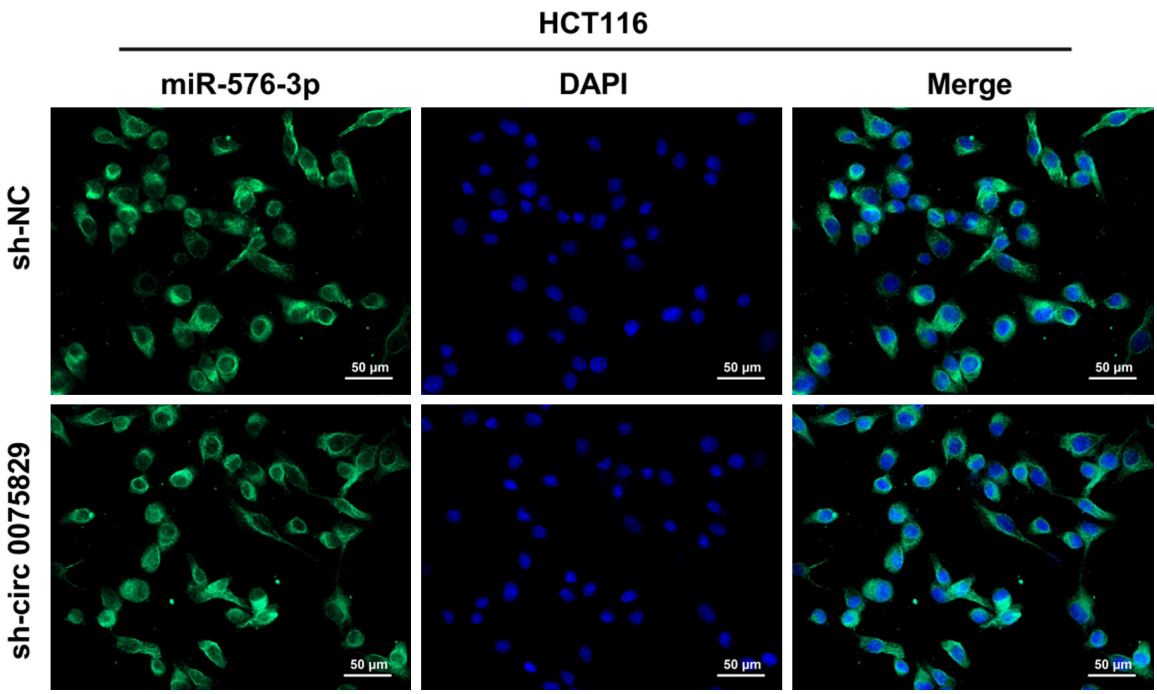

Supplementary Figure 1. Localization of miR-576-3p in HCT116 cells. Localization of miR-576-3p by FISH after HCT116 cells were transfected with sh-circ_0075829. Magnification: ×400, Scale bar =50 μm.

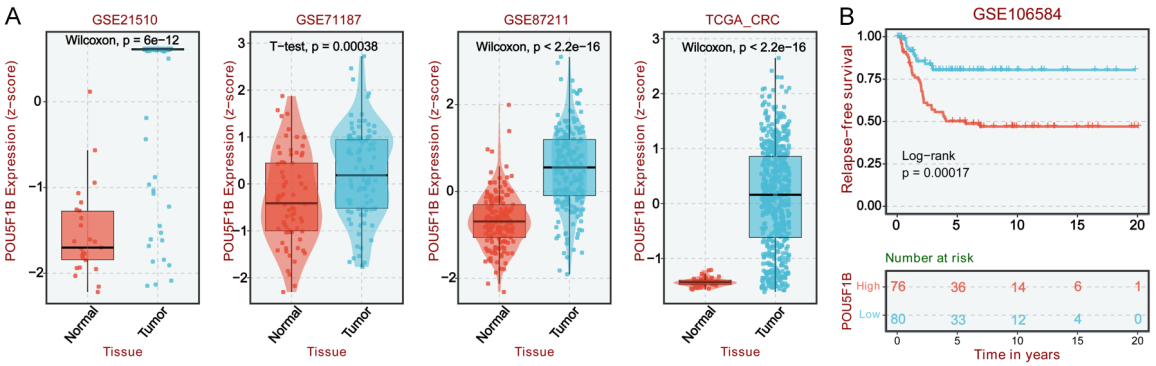

Supplementary Figure 2. High expression of POU5F1B indicated a short RFS in colon cancer patients. A. Expression of POU5F1B based on the GSE21510, GSE71187, GSE87211 microarray dataset, and TCGA_CRC databases. B. The RFS of patients with CRC was assessed by the kmplot website based on GSE106584 microarray dataset.